Inorganic Chemistry

Article

pubs.acs.org/IC

Synthesis and Characterization of Eight Compounds of the MU_8Q_{17} Family: ScU_8S_{17}, CoU_8S_{17}, NiU_8S_{17}, TiU_8Se_{17}, VU_8Se_{17}, CrU_8Se_{17}, CoU_8Se_{17}, and NiU_8Se_{17}

Matthew D. Ward,[†] Adel Mesbah,[†] Stefan G. Minasian,[‡] David K. Shuh,[‡] Tolek Tyliszczak,[§] Minseong Lee,[⊥] Eun Sang Choi,[⊥] Sébastien Lebègue,[∥] and James A. Ibers*[,†]

[†]Department of Chemistry, Northwestern University, Evanston, Illinois 60208−3113, United States

[‡]Chemical Sciences Division, MS70A1150, and [§]Advanced Light Source, MS6R2100, Lawrence Berkeley National Laboratory, Berkeley, California 94720, United States

[⊥]Department of Physics and National High Magnetic Field Laboratory, Florida State University, Tallahassee, Florida 32310-3706, United States

[∥]Laboratoire de Cristallographie, Résonance Magnétique, et Modélisations CRM2 (UMR UHP-CNRS 7036), Faculté des Sciences et Techniques, Université de Lorraine, BP 70239, Boulevard des Aiguillettes, 54506 Vandoeuvre-lès-Nancy Cedex, France

Supporting Information

ABSTRACT: The solid-state MU_8Q_{17} compounds ScU_8S_{17}, CoU_8S_{17}, NiU_8S_{17}, TiU_8Se_{17}, VU_8Se_{17}, CrU_8Se_{17}, CoU_8Se_{17}, and NiU_8Se_{17} were synthesized from the reactions of the elements at 1173 or 1123 K. These isostructural compounds crystallize in space group C_{2h}^3 - $C2/m$ of the monoclinic system in the CrU_8S_{17} structure type. X-ray absorption near-edge structure spectroscopic studies of ScU_8S_{17} indicate that it contains Sc^{3+}, and hence charge balance is achieved with a composition that includes U^{3+} as well as U^{4+}. The other compounds charge balance with M^{2+} and U^{4+}. Magnetic susceptibility measurements on ScU_8S_{17} indicate antiferromagnetic couplings and a highly reduced effective magnetic moment. Ab Initio calculations find the compound to be metallic. Surprisingly, the Sc−S distances are actually longer than all the other M−S interactions, even though the ionic radii of Sc^{3+}, low-spin Cr^{2+}, and Ni^{2+} are similar.

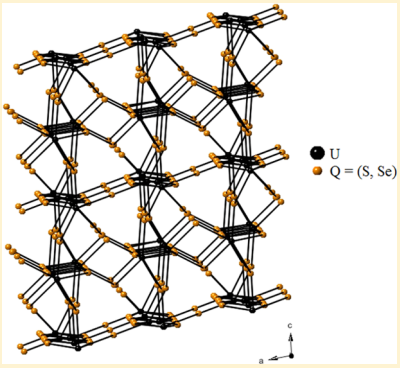

INTRODUCTION

Ternary uranium(IV) chalcogenides (Q = S, Se, Te) are a well studied family of compounds, and many of these compounds exhibit interesting physical properties based upon the f^2 configuration of U^{4+}.[1,2] Most such compounds are rationally charge balanced with U^{4+}. However, ScU_3S_6,[3] $ScUS_3$,[4,5] and the binary UTe_2[6] have been reported to contain U^{3+}. There are also some chalcogenides that contain both U^{3+} and U^{4+}; these include U_3Q_5 (Q = S, Se, Te),[7−9] UMo_6Q_8 (Q = S, Se),[10] and $U_xPd_3S_4$ ($0.9 < x < 1.0$).[11] The stability of U^{4+} makes it difficult to synthesize compounds with U^{3+}, but exploration of systems with the f^3 configuration could offer physical properties different from those with the f^2 configuration.

A number of members of the MU_8Q_{17} (M = 3d transition metal; Q = S, Se) family of compounds have been synthesized and their structures inferred from X-ray powder diffraction studies[12−14] or from single-crystal diffraction data on the sulfides.[15−18] These compounds all adopt the CrU_8S_{17} structure type.[15] Because there are no Q−Q bonds in these structures, charge balance is achieved with +4 and −2 for U and Q, respectively, if M is presumed to be +2. Magnetic studies on powders of Mg and Ti−Ni for both the sulfides and selenides indicated induced antiferromagnetism.[19] These studies are consistent with M^{2+} but do not rule out M^{3+}. In particular the existence of ScU_8S_{17},[18] in which Sc^{3+} would be expected, engenders the possibility that some compounds in this family might contain U^{3+} in addition to U^{4+}.

Here we report the syntheses of single crystals and the crystal structures of three sulfides and five selenides, namely, ScU_8S_{17}, CoU_8S_{17}, NiU_8S_{17}, TiU_8Se_{17}, VU_8Se_{17}, CrU_8Se_{17}, CoU_8Se_{17}, and NiU_8Se_{17}. We also report XANES results, magnetic results, and ab initio calculations for ScU_8S_{17}.

EXPERIMENTAL METHODS

Syntheses. Black needles of MU_8Q_{17} were obtained by high-temperature solid-state reactions of the elements. Reactions were loaded into carbon-coated fused-silica tubes under an inert Ar atmosphere. The tubes were then evacuated to 10^{-4} Torr and flame-sealed. The following reagents were used as received: Sc (Alfa Aesar 99.8%), Ti (Alfa 99.5%), V (Johnson Matthey 99.5%), Cr (Alfa Aesar 99.99%), Co (Alfa Aesar 99%), Ni (Alfa Aesar 99.5%), S (Mallinckrodt 99.6%), Se (Cerac 99.999%), KCl (Omnipur 99−100%), RbCl (Alfa 99.8%), CsCl (MP Biomedicals 99.9%). Depleted U turnings (Oak Ridge National Laboratory) were powdered by hydridization, and the

Received: March 31, 2014
Published: June 16, 2014

   dx.doi.org/10.1021/ic500721d | Inorg. Chem. 2014, 53, 6920−6927

Table 1. Crystallographic Details for the Present MU_8Q_{17} Compounds[a]

compound	ScU_8S_{17}	CoU_8S_{17}	NiU_8S_{17}	TiU_8Se_{17}	VU_8Se_{17}	CrU_8Se_{17}	CoU_8Se_{17}	NiU_8Se_{17}
a (Å)	13.3559(4)	13.3045 (5)	13.2685 (6)	13.8890 (4)	13.9192 (4)	13.8485(5)	13.8743 (7)	13.8851 (4)
b (Å)	8.4468(2)	8.3634 (3)	8.3504 (3)	8.8141 (2)	8.7569 (2)	8.7846(3)	8.7194 (4)	8.8016 (2)
c (Å)	10.5455(3)	10.4079 (4)	10.3797 (5)	10.8876 (3)	10.8758 (3)	10.8795(4)	10.8342 (5)	10.8799 (3)
V /Å^3	1165.67(6)	1134.56 (7)	1126.80 (8)	1306.70 (6)	1298.75 (6)	1295.90 (8)	1282.98 (11)	1303.41 (6)
β (deg)	101.533(1)	101.571 (2)	101.538 (2)	101.369 (1)	101.561 (1)	101.728(2)	101.798 (2)	101.401 (1)
$R(F)^b$	0.022	0.019	0.030	0.023	0.021	0.026	0.029	0.033
$R_w(F_o^2)^c$	0.051	0.041	0.086	0.065	0.046	0.060	0.084	0.095
q^d	0.0184	0.0059	0.0568	0.0357	0.0204	0.0287	0.0283	0.0565

[a]Monoclinic space group C_{2h}^3 - $C2/m$; $Z = 2$; $T = 100(2)$ K. [b]$R(F) = \Sigma||F_o| - |F_c||/\Sigma|F_o|$ for $F_o^2 > 2\sigma(F_o^2)$. [c]$R_w(F_o^2) = \{\Sigma [w(F_o^2 - F_c^2)^2]/\Sigma wF_o^4\}^{1/2}$ for all data. [d]$w^{-1} = \sigma^2(F_o^2) + (qF_o^2)^2$ for $F_o^2 \geq 0$; $w^{-1} = \sigma^2(F_o^2)$ for $F_o^2 < 0$.

resultant hydride was decomposed by heating under a vacuum in a modification[20] of a previous literature procedure.[21]

ScU_8S_{17} was synthesized from the reaction of U (0.126 mmol), Sc (0.126 mmol), S (0.378 mmol), and CsCl (0.594 mmol). The reaction was heated to 1173 K in 12 h, held at 1173 K for 6 h, cooled to 1073 K in 12 h, and held there for 96 h. The reaction was then cooled to 773 K over 150 h and finally to 298 K in a further 48 h.

MU_8S_{17} (M = Co, Ni) were obtained from the reactions of U (0.130 mmol), M (0.130 mmol), S (0.5 mmol), and RbCl (0.83 mmol). The reactions were heated to 1123 K in 24 h, held for 168 h, cooled to 473 K in 150 h, and finally cooled to 298 K in 24 h.

MU_8Se_{17} (M = Ti, Cr, Ni) were synthesized from the reactions of U (0.126 mmol), M (0.126 mmol), Se (0.378 mmol), and CsCl (0.2969 mmol). The reactions were heated to 1173 K in 12 h, held at 1173 K for 6 h, cooled to 1073 K in 12 h, and held there for 96 h. The reactions were then cooled to 773 K in 60 h and finally to 298 K in a further 12 h.

VU_8Se_{17} was synthesized from the reaction of U (0.126 mmol), V (0.126 mmol), Se (0.378 mmol), and CsCl (0.4454 mmol) when heated as for MU_8Se_{17}.

CoU_8Se_{17} was obtained by the reaction of U (0.130 mmol), Co (0.130 mmol), Se (0.5 mmol), and KCl (0.83 mmol) when heated as for MU_8Se_{17}.

These reactions yielded black needles that were manually extracted for analysis. The products also contained black powder and in some cases other crystalline phases. Although the reactions were initially loaded with reactants in the stoichiometric ratio M:U:Q = 1:1:3 in an effort to produce compounds of the composition MUQ_3, in fact the major products were MU_8Q_{17} except for TiU_8Se_{17} and CrU_8Se_{17}. In these latter reactions, the major product was $Cs_2U_6M_2Se_{15}$[22] with MU_8Se_{17} as a minor product. Additional phases that were found in all reactions included U/Q binaries, M/Q binaries, and excess ACl flux. Elemental analysis of the selected crystals using an Hitachi 3400 SEM equipped for EDX analysis showed the presence of only U, M, and Q.

Structure Determinations. Single-crystal X-ray diffraction data were collected at 100(2) K using graphite-monochromatized MoKα radiation (λ = 0.71073 Å) on a Bruker APEX2 diffractometer.[23] The crystal to detector distance was 60 mm; the exposure time was 10 s/frame. Collection of intensity data, cell refinement, and data reduction were performed using APEX2 as a series of 0.3° scans in φ and ω.[23] Face-indexed absorption, incident beam, and decay corrections were performed by the program SADABS[24] for ScU_8S_{17}, VU_8Se_{17}, and CoU_8Se_{17}. The program TWINABS[25] was used to make absorption, incident beam, and decay corrections for TiU_8Se_{17}, CrU_8Se_{17}, CoU_8S_{17}, NiU_8S_{17}, and NiU_8Se_{17}. For each of these compounds a second domain was found related to the first one by the twin law 1 0 0.5 0 −1 0 0 0 −1. These secondary domains were refined and make up 30.5(1)%, 14.4(1)%, 3.5(1)%, 46.8(1)%, and 25.8(1)% of the crystal, respectively, for TiU_8Se_{17}, CrU_8Se_{17}, CoU_8S_{17}, NiU_8S_{17}, and NiU_8Se_{17}. The crystal structures were solved and refined with the use of the Shelx-14 algorithms of the SHELXT program package.[24,26] Atom positions were standardized using the program STRUCTURE TIDY.[27] Crystallographic images were made using the program CRYSTALMAKER.[28] Further details are given in Table 1 and Supporting Information.

XANES Measurements. XANES spectra for ScU_8S_{17} were collected in transmission mode using the STXM at the Molecular Environmental Sciences (MES) elliptically polarizing undulator beamline 11.0.2 at the Advanced Light Source (ALS), which is operated in topoff mode at 500 mA, in a ∼0.5 atm He filled chamber.[29] Samples for STXM measurements were encapsulated between two 100 nm Si_3N_4 membranes (Silson). Energy calibrations were performed at the Ne K-edge for Ne (867.3 eV), the O K-edge for CO_2 (538.90 eV), and the C K-edge for CO_2 (294.95 eV). The energy resolution (fwhm) was estimated to be better than 0.2 eV, and spectra were collected using linearly polarized radiation. Spectra at each image pixel or particular regions of interest in the sample image were extracted from the "stack", which is a collection of images recorded at multiple, closely spaced photon energies across the absorption edge.[30−32] Determination of the U $N_{5,4}$-edge branching ratios followed standard data analysis procedures, described previously.[29,33−35]

Magnetic Susceptibility Measurements. Magnetic properties of ScU_8S_{17} were investigated by performing magnetic susceptibility and magnetization measurements with a commercial SQUID magnetometer (Quantum Design MPMS). The ground single-crystal sample (total mass 2.29 mg) was attached on a quartz rod with vacuum grease. The data were taken under zero field-cooled (ZFC) and then field-cooled (FC) upon warming up after the sample was cooled from T = 300 K without and with external field, respectively.

Ab Initio Calculations. The calculations were performed with the Vienna ab Initio Simulation Package,[36,37] implementing density functional theory[38,39] with the projector augmented wave method.[40] We have used the default cutoff for the plane-wave part of the wave function and a 6 × 6 × 6 mesh for the integrations over the Brillouin zone. The generalized gradient approximation[41] was used as the exchange-correlation functional, together with spin polarization. The experimental geometry was used for the structure. Because the magnetic coupling was identified as antiferromagnetic from susceptibility measurements, we have tried all the possible antiferromagnetically ordered ground states at zero temperature in the crystal cell and compared their total energies, the one with the lowest energy being identified as the ground-state magnetic configuration.

RESULTS

Syntheses. The MU_8Q_{17} compounds ScU_8S_{17}, CoU_8S_{17}, NiU_8S_{17}, TiU_8Se_{17}, VU_8Se_{17}, CrU_8Se_{17}, CoU_8Se_{17}, and NiU_8Se_{17} were synthesized from the reactions of the elements in an ACl flux at 1173 or 1123 K. The reactions yielded black needles of MU_8Q_{17} as the major product in all cases except when M = Ti or Cr, when the major products were black prisms of $Cs_2U_6M_2Se_{15}$.[22] Previously, single crystals of MnU_8S_{17}[17] were synthesized from the reaction of the elements in an RbCl flux at 1073 K and powders and single crystals of other MU_8Q_{17} compounds were synthesized by the reaction of UQ_2, M, and Q in the appropriate stoichiometries at $T \geq 1423$ K.[12−15,19]

dx.doi.org/10.1021/ic500721d | Inorg. Chem. 2014, 53, 6920−6927

Crystal Structure of MU_8Q_{17}. All reported structures of the MU_8Q_{17} family crystallize in the CrU_8S_{17} structure type[15] in the monoclinic space group C_{2h}^3 - $C2/m$. These include the eight compounds reported here and the earlier single-crystal studies of the sulfides.[15−17] The asymmetric unit of this structure type is composed of the following atoms with their appropriate site symmetries: U1 (1), U2 (m), U3 (m), Q1 (1), Q2 (1), Q3 (m), Q4 (m), Q5 (m), Q6 (m), Q7 ($2/m$), and M1 ($2/m$). Each U atom is coordinated by eight Q atoms in a bicapped trigonal-prismatic arrangement, and the M atom is coordinated by six Q atoms in a distorted octahedral environment. Each M atom has two short M−Q bonds 180° apart and four longer equatorial M−Q bonds. Each U1 atom face shares with two other U1 atoms and corner shares with a third U1 atom to form U_4Q_{21} units. These units then edge share to form infinite chains in the [010] direction. The U2 and U3 sites form a three-dimensional infinite framework with two types of channels along [010] (Figure 1). The U1 chains insert into the larger channel, whereas the M atoms insert into the smaller channel (Figure 2).

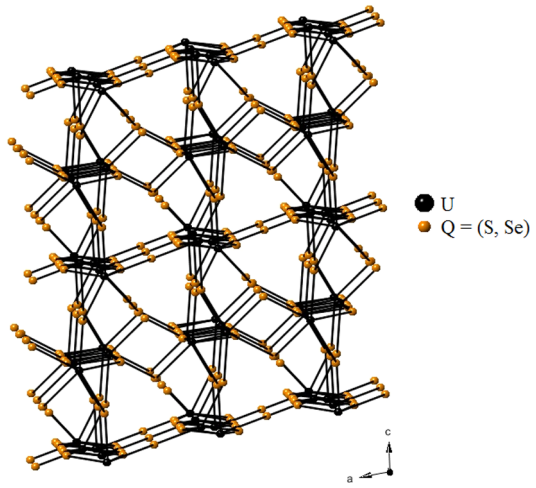

Figure 1. Three dimensional framework formed by the U(2) and U(3) sites in the MU_8Se_{17} compounds.

The single-crystal structures of TiU_8Se_{17}, VU_8Se_{17}, CrU_8Se_{17}, CoU_8Se_{17}, and NiU_8Se_{17} are the first selenide members of the MU_8Q_{17} family to be reported. The U−Se interatomic distances (Table 2) are correspondingly longer than seen for U−S distances and range from 2.865(1) Å to 3.077(1) Å for U(1)−Se, 2.858(1) Å to 2.946(1) Å for U(2)−Se, and 2.802(1) Å to 3.115(1) Å for U(3)−Se. These distances compare favorably with those seen in $UFeSe_3$,[42] which is a compound of U^{4+} and Fe^{2+} and has U−Se interatomic distances from 2.886(1) Å to 3.117(1) Å.

The M−Se interatomic distances range from 2.415(1) Å to 2.469(1) Å for M−Se3 and from 2.541(1) Å to 2.569(1) Å for M−Se2. As expected, the M−Se distances are correspondingly longer than those for M−S. The series follows the expected trend of decreasing distances from Ti to Co with a small increase at Ni.

For MU_8S_{17}, the interatomic distances are shown in Table 3. The interatomic distances range from 2.729(1) Å to 2.955(1) Å for U1−S, 2.735(1) Å to 2.867(1) Å for U2−S, and 2.680(1) Å to 3.033(1) Å for U3−S. These distances compare favorably with those seen in the MUS_3[4,42,43] compounds in which U is also coordinated by eight S atoms in a bicapped trigonal-prismatic arrangement. The M−S interatomic distances in MU_8S_{17} range from 2.302(1) Å to 2.434(1) Å for M−S3 and from 2.434(1) Å to 2.520(1) Å for M−S2. These distances again compare favorably with those in MUS_3,[4,42,43] which also has $M^{2+}S_6$ octahedra.

Surprisingly, Table 3 shows that the Sc−S distances are actually longer than all the other M−S interactions, even though the ionic radii of Sc^{3+}, low-spin Cr^{2+}, and Ni^{2+} are similar, namely, 0.885 Å, 0.87 Å, and 0.83 Å, respectively.[44] Compare these Sc−S interatomic distances in ScU_8S_{17} of 2.434(1) Å and 2.520(1) Å with those seen in $ScUS_3$[4,5] of 2.490(2) Å and 2.603(2) Å and ScU_3S_6[3] of 2.439(6) Å and 2.598(4) Å. The latter compounds purportedly contain Sc^{3+} and U^{3+}.

In contrast, the U−S interatomic distances for ScU_8S_{17} are similar to those for the other MU_8S_{17} structures where the metal site is charge-balanced with U^{4+} and M^{2+}. If ScU_8S_{17} contains Sc^{3+} then charge balance is achieved with one U^{3+} and seven U^{4+}. Although in these compounds an eight-coordinate U^{3+}−S distance would be expected to exceed that of an eight-

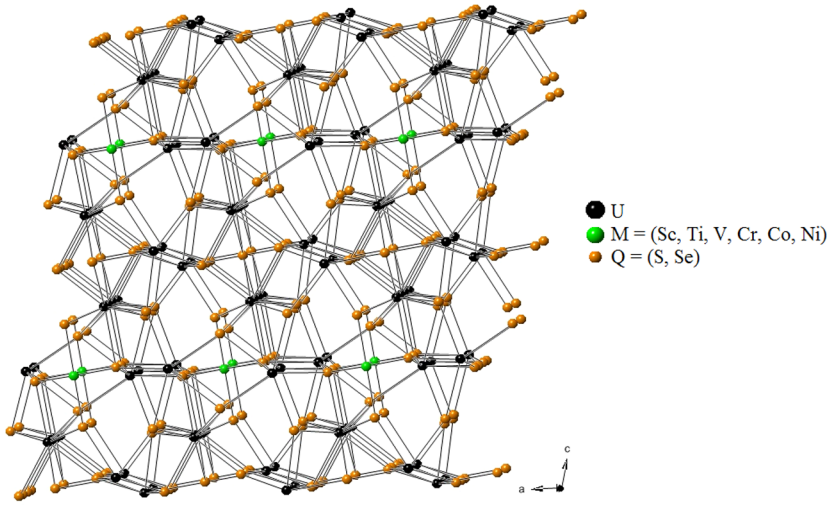

Figure 2. Packing in the MU_8Q_{17} structure.

dx.doi.org/10.1021/ic500721d | Inorg. Chem. 2014, 53, 6920−6927

Table 2. Selected Interatomic Distances (Å)[a] for MU_8Se_{17} Compounds

	TiU_8Se_{17}	VU_8Se_{17}	CrU_8Se_{17}	CoU_8Se_{17}	NiU_8Se_{17}
T (K)	100	100	100	100	100
U1−Se1	2.927(1)	2.930(1)	2.920(1)	2.919(1)	2.925(1)
U1−Se1	2.979(1)	2.987(1)	2.970(1)	2.969(1)	2.978(1)
U1−Se2	2.963(1)	2.928(1)	2.970(1)	2.911(1)	2.956(1)
U1−Se3	2.894(1)	2.874(1)	2.878(1)	2.865(1)	2.891(1)
U1−Se4	2.991(1)	2.982(1)	2.985(1)	2.972(1)	2.988(1)
U1−Se5	2.952(1)	2.944(1)	2.945(1)	2.932(1)	2.948(1)
U1−Se6	2.994(1)	2.968(1)	2.995(1)	2.957(1)	2.988(1)
U1−Se7	3.077(1)	3.074(1)	3.065(1)	3.060(1)	3.075(1)
U2−Se1 × 2	2.890(1)	2.890(1)	2.884(1)	2.878(1)	2.889(1)
U2−Se1 × 2	2.902(1)	2.897(1)	2.897(1)	2.891(1)	2.900(1)
U2−Se3	2.873(1)	2.862(1)	2.886(1)	2.862(1)	2.870(1)
U2−Se4	2.875(1)	2.869(1)	2.877(1)	2.858(1)	2.872(1)
U2−Se5	2.917(1)	2.910(1)	2.897(1)	2.888(1)	2.914(1)
U2−Se7	2.943(1)	2.946(1)	2.945(1)	2.935(1)	2.942(1)
U3−Se2 × 2	2.816(1)	2.809(1)	2.835(1)	2.802(1)	2.812(1)
U3−Se2 × 2	3.057(1)	3.035(1)	3.048(1)	3.024(1)	3.053(1)
U3−Se4	2.913(1)	2.916(1)	2.903(1)	2.905(1)	2.913(1)
U3−Se5	2.920(1)	2.923(1)	2.926(1)	2.913(1)	2.919(1)
U3−Se6	3.005(1)	3.030(1)	2.994(1)	3.034(1)	3.007(1)
U3−Se6	3.096(1)	3.115(1)	3.070(1)	3.101(1)	3.096(1)
M−Se3 × 2	2.469(1)	2.453(1)	2.427(1)	2.415(1)	2.465(1)
M−Se2 × 4	2.569(1)	2.569(1)	2.541(1)	2.557(1)	2.569(1)

[a]All interatomic distances have been rounded to three significant figures.

Table 3. Selected Interatomic Distances (Å)[a] for MU_8S_{17} Compounds

	ScU_8S_{17}	CrU_8S_{17}[b]	MnU_8S_{17}[c]	FeU_8S_{17}[d]	CoU_8S_{17}	NiU_8S_{17}
T (K)	100	RT	100	RT	100	100
U1−S1	2.798(1)	2.788	2.802(2)	2.798	2.799(1)	2.792(2)
U1−S1	2.839(1)	2.842	2.847(2)	2.855	2.864(1)	2.846(2)
U1−S2	2.821(1)	2.829	2.762(2)	2.790	2.766(1)	2.774(2)
U1−S3	2.784(1)	2.760	2.755(2)	2.751	2.741(1)	2.729(2)
U1−S4	2.867(1)	2.867	2.852(2)	2.857	2.844(1)	2.848(2)
U1−S5	2.819(1)	2.815	2.813(2)	2.821	2.812(1)	2.806(2)
U1−S6	2.878(1)	2.845	2.839(2)	2.834	2.819(2)	2.809(2)
U1−S7	2.950(1)	2.954	2.951(1)	2.955	2.945(1)	2.941(1)
U2−S1 × 2	2.756(1)	2.760	2.763(2)	2.765	2.760(2)	2.756(2)
U2−S1 × 2	2.784(1)	2.782	2.768(2)	2.778	2.762(1)	2.761(2)
U2−S3	2.749(1)	2.772	2.735(3)	2.760	2.751(2)	2.758(3)
U2−S4	2.763(1)	2.769	2.747(3)	2.766	2.748(2)	2.751(3)
U2−S5	2.811(1)	2.774	2.791(3)	2.775	2.764(2)	2.765(3)
U2−S7	2.867(1)	2.856	2.856(1)	2.851	2.843(1)	2.835(1)
U3−S2 × 2	2.693(1)	2.721	2.680(2)	2.709	2.690(1)	2.693(2)
U3−S2 × 2	2.922(1)	2.922	2.896(2)	2.905	2.894(1)	2.896(2)
U3−S4	2.819(1)	2.761	2.819(3)	2.788	2.789(2)	2.771(3)
U3−S5	2.857(1)	2.814	2.841(3)	2.823	2.808(2)	2.789(3)
U3−S6	2.888(1)	2.868	2.912(3)	2.897	2.900(2)	2.891(3)
U3−S6	2.994(1)	2.994	3.031(3)	3.033	3.021(2)	3.019(3)
M−S3 × 2	2.434(1)	2.326	2.398(3)	2.343	2.328(2)	2.302(3)
M−S2 × 4	2.520(1)	2.434	2.517(2)	2.461	2.465(1)	2.439(2)

[a]All interatomic distances have been rounded to three significant figures. [b]Ref 15. [c]Ref 17. [d]Ref 16.

coordinate U^{4+}−S distance by about 0.14 Å,[45] if the distribution of the U^{3+} atom were random or nearly so over the three crystallographically independent U sites then the effect on the U−S distances would be minimal. As calculated in Platon,[46] bond valence analysis,[47] a strictly empirical method, led to valences of atoms U1, U2, U3, and M that ranged from 3.6 to 4.1, 4.3 to 4.9, 3.7 to 4.1, and 1.7 to 4.0, respectively. Because the metrical results for MU_8S_{17} did not enable us to resolve how to charge balance ScU_8S_{17}, we turned to X-ray absorption near-edge structure (XANES) measurements.

XANES Spectroscopy. A soft X-ray scanning transmission X-ray microscope (STXM) was used to record Sc $L_{3,2}$-edge and U $N_{5,4}$-edge XANES spectra to corroborate the structural and magnetic results. Scandium $L_{3,2}$ ($2p_{3/2,1/2}$)-edge XANES has

dx.doi.org/10.1021/ic500721d | Inorg. Chem. 2014, 53, 6920−6927

been used to characterize Sc thin films as well as compounds.[48−50] The linear background-subtracted Sc $L_{3,2}$-edge spectrum for ScU_8S_{17} is shown in Figure 3. The data are in

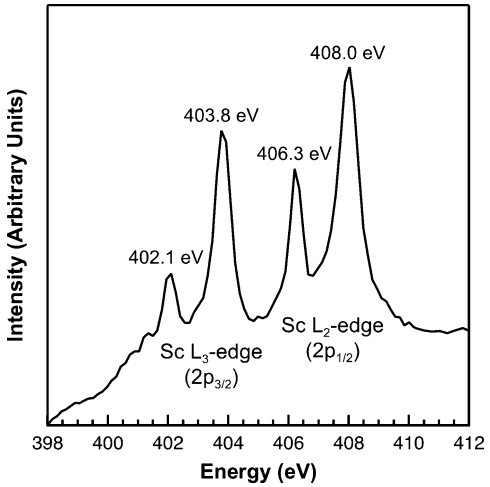

Figure 3. Sc $L_{3,2}$-edge XANES spectra for ScU_8S_{17}.

close agreement with those published previously for d^0 Sc_2O_3 and ScF_3.[48] For a d^0 Sc species, the $L_{3,2}$-edge features arise from dipole-allowed $2p^63d^0 \rightarrow 2p^53d^1$ transitions, which are separated by approximately 4 eV into two primary L_3 ($2p_{3/2}$) and L_2 ($2p_{1/2}$) edges resulting from spin−orbit splitting. The peak maxima observed for ScU_8S_{17} were found at 402.1 and 403.8 eV for the L_3-edge, and 406.3 and 408.0 for the L_2-edge, giving a L_3−L_2 edge splitting of 4.2 eV. For comparison peak maxima were interpolated from the published spectrum of ScF_3,[43] and found at 402.4 and 404.3 for the L_3-edge, and 406.7 and 408.5 for the L_2-edge ($L_3 - L_2$ = 4.2 eV). The energy splitting between the two L_3 peaks and two L_2 peaks was measured at 1.7 eV at each edge for ScU_8S_{17}, which also compares well with published energy splittings for ScF_3 (1.9 eV at the L_3-edge and 1.8 eV at the L_2-edge). Overall, the close correspondence between the spectral profile and peak splittings provides confidence in assigning a d^0 electronic configuration to the Sc atoms in ScU_8S_{17}.

XANES spectra from the U $N_{5,4}$-edges were collected to establish the oxidation state of the U in ScU_8S_{17}, as the electronic excitations from the 4d core levels directly probe orbitals with 5f character.[33,34,51,52] Background-subtracted U $N_{5,4}$-edge XANES spectra for ScU_8S_{17} have been included in Figure 4. The $N_{5,4}$-edge absorptions arise from dipole allowed $4d^{10}5f^n \rightarrow 4d^95f^{n+1}$ transitions, which were split by 41.4 eV into two primary U N_5 (736.7 eV) and N_4 (778.2 eV) edges because of spin−orbit coupling. The N_5 and N_4 edge energies fall into a regime that has been observed for a variety of U^{3+} and U^{4+} complexes and materials.[34,53] Previous studies have shown that the branching ratio of N_5 and N_4 features can be sensitive to changes in valence electronic structure.[54−57] As shown by a graphical analysis of the second derivative of the raw spectra,[56] the branching ratio $A_5/(A_5 + A_4)$ was 0.69, where A_5 and A_4 are the areas under the N_5 and N_4 peaks (Figure 4 inset). This value is similar to those observed previously for U^{4+} compounds such as $U(C_8H_8)_2$ (0.67),[35] $RbAuUSe_3$ (0.69),[33,58] and UF_4 (0.68).[54] Although additional U $N_{5,4}$-edge spectroscopic measurements on a broad series of molecular and solid-state uranium compounds is needed to fully validate this interpretation, the XANES results are

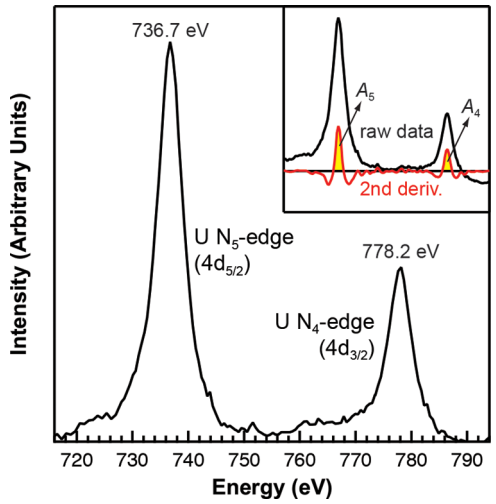

Figure 4. U $N_{5,4}$-edge XANES spectra for ScU_8S_{17}. An additional plot (inset) shows how the area beneath each peak was determined graphically from the second derivative of the raw data.[56]

consistent with a formal oxidation state of the U atoms in ScU_8S_{17} that is close to +4 and is compatible with that of 3.9 necessary to achieve charge balance.

Magnetic Susceptibility. Figure 5 shows the temperature dependence of magnetic susceptibility (χ) of ScU_8S_{17} for H =

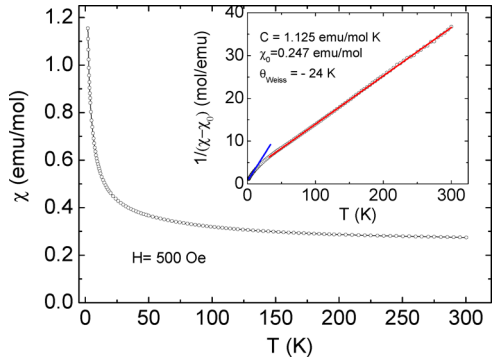

Figure 5. Temperature dependence of magnetic susceptibility of ScU_8S_{17} for H = 500 Oe. The inset shows inverse magnetic susceptibility.

500 Oe. There is no difference between ZFC and FC data. In the entire measured temperature range (2 K ≤ T ≤ 300 K), $\chi(T)$ decreases with temperature reminiscent of the Curie law. It is notable that χ shows very weak temperature dependence near room temperature and has a large positive value. The measured moment (1.2×10^{-4} emu) is much larger than the diamagnetic contribution from the sample holder ($\sim -1 \times 10^{-6}$ emu) or from the core electrons (Pascal's constant $\sim -4 \times 10^{-7}$ emu) for the given sample mass and magnetic field.

We fitted the high-temperature data (40 K ≤ T ≤ 300 K) with the modified Curie−Weiss Law, and the resulting inverse magnetic susceptibility ($1/(\chi - \chi_0)$) is shown in the inset of Figure 5. The modified Curie−Weiss Law can be expressed as $\chi = C/(T - \theta) + \chi_0$, where C is the Curie constant, χ_0 is the temperature independent susceptibility, and θ is the Weiss temperature. The inverse magnetic susceptibility is linear at high temperatures as expected from the fitting procedure whereas deviation from linearity is apparent at lower temperatures. From the slope of the high-temperature region, the

dx.doi.org/10.1021/ic500721d | Inorg. Chem. 2014, 53, 6920−6927

effective magnetic moment (μ_{eff}) is found to be 3.00(3) μ_B, which decreases to 2.0(1) μ_B below T = 7 K. θ is estimated to be −24(1) K and χ_0 = 0.247(5) emu/mol at the high temperature region.

The μ_{eff} at high temperatures is between those of free ionic U^{3+} (3.62 μ_B) or U^{4+} (3.58 μ_B) and U^{5+} (2.54 μ_B) in the L−S scheme. The negative θ suggests antiferromagnetic coupling between magnetic ions. The overall temperature dependence and the reduced effective moment are similar to those of MgU_8Se_{17},[19] where U is the only source of the magnetic moment. A large and negative θ (−60 K) but no magnetic ordering was also observed in MgU_8Se_{17}. The above observations can be explained by the crystalline electric field (CEF) effect, where the degeneracy of Hund's multiplet ($^4I_{9/2}$ for U^{3+}, $^3H_4$ for U^{4+}) is lifted by the crystal field. Even further decrease of μ_{eff} at lower temperature can also be explained by the CEF effect if the CEF energy level splitting is close to the measured temperature range.

Another possible explanation for the reduced effective moment is itinerant magnetism of 5f electrons.[59] This explanation is partly consistent with the positive temperature independent magnetic susceptibility (χ_0). Its positive value can be either from ferromagnetism or Pauli paramagnetism from itinerant electrons. Ferromagnetism is not obvious from the magnetization data (Figure 6). Note that the magnitude of χ_0 is about 2 orders of magnitude larger than that of typical actinide metals.[59] If the itinerant magnetism should be relevant, the absence of the magnetic ordering in spite of the large θ could be ascribed to the disordered nature of U (coexistence of U^{3+} and U^{4+}). All U−U distances in the structures are beyond the Hill limit of magnetic ordering.

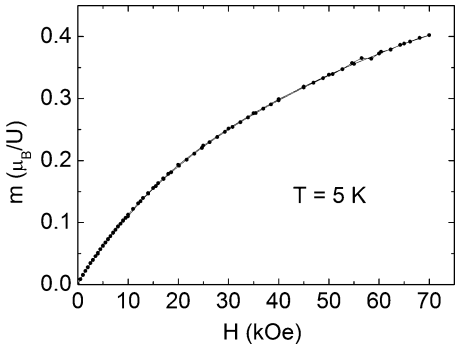

Figure 6. Magnetization data of ScU_8S_{17} at T = 5 K. Both up and down sweep curves are shown.

Ab Initio Calculations. We have chosen to focus on the electronic structure of ScU_8S_{17} as the example of the electronic structure of the MU_8Q_{17} family of compounds. The total and partial density of states (PDOS) of ScU_8S_{17} is presented in Figure 7,with the total density of states showing no net spin polarization, as expected for an antiferromagnetically ordered material. The compound is found to be metallic, with a finite density of states at the Fermi level. Also, the strong spin polarization of the U atoms induces a small spin polarization of the Sc and S species, as their density of states is not completely symmetric with respect to spin. The states at the Fermi level originate almost exclusively from U-f states, with a small contribution from Sc-d states.

CONCLUSIONS

The solid-state MU_8Q_{17} compounds ScU_8S_{17}, CoU_8S_{17}, NiU_8S_{17}, TiU_8Se_{17}, VU_8Se_{17}, CrU_8Se_{17}, CoU_8Se_{17}, and NiU_8Se_{17} were synthesized from the reactions of the elements at 1173 or 1123 K. These isostructural compounds crystallize in space group C_{2h}^3 - $C2/m$ of the monoclinic system in the CrU_8S_{17} structure type. XANES spectroscopic studies of ScU_8S_{17} indicate that it contains Sc^{3+}, and hence charge balance is achieved with a composition that includes U^{3+} as well as U^{4+}. The other compounds charge balance with M^{2+} and U^{4+}. Surprisingly, the Sc−S distances are actually longer than all the other M−S interactions, even though the ionic radii of Sc^{3+}, low-spin Cr^{2+}, and Ni^{2+} are similar. Magnetic susceptibility measurements on ScU_8S_{17} indicate that it has an antiferromagnetic interaction with a highly reduced effective magnetic moment. Ab Initio calculations find the compound to be metallic. The states at the Fermi level originate almost exclusively from U-f states.

ASSOCIATED CONTENT

Supporting Information

Crystallographic file in CIF format for ScU_8S_{17}, CoU_8S_{17}, NiU_8S_{17}, TiU_8Se_{17}, VU_8Se_{17}, CrU_8Se_{17}, CoU_8Se_{17}, and NiU_8Se_{17}. This material is available free of charge via the Internet at http://pubs.acs.org

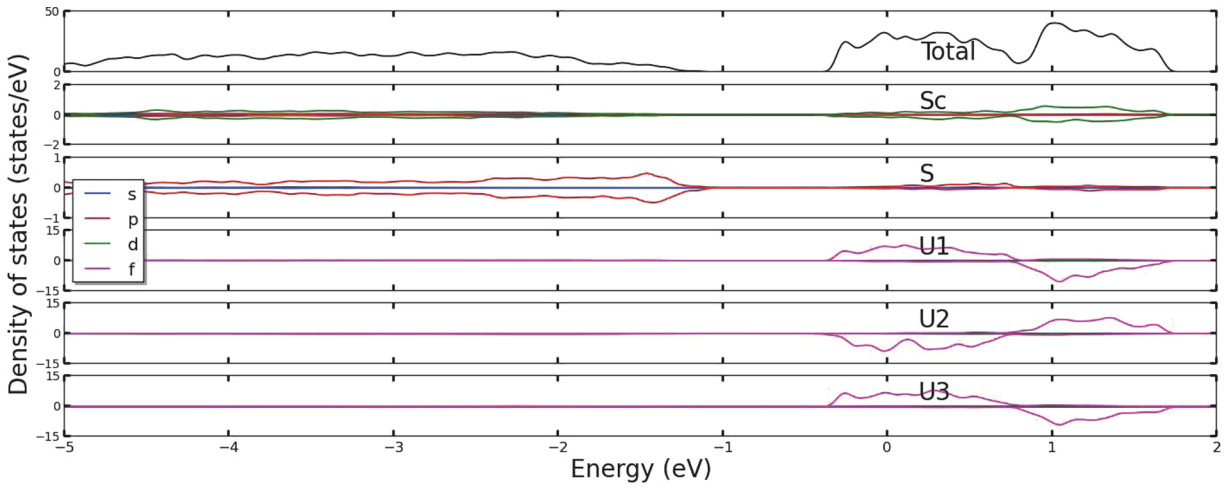

Figure 7. Total and partial density of states (PDOS) of ScU_8S_{17}.

dx.doi.org/10.1021/ic500721d | Inorg. Chem. 2014, 53, 6920−6927

AUTHOR INFORMATION

Corresponding Author

*E-mail: ibers@chem.northwestern.edu.

Notes

The authors declare no competing financial interest.

ACKNOWLEDGMENTS

This research was supported at Northwestern University by the U.S. Department of Energy, Basic Energy Sciences, Chemical Sciences, Biosciences and Geosciences Division and Division of Materials Science and Engineering Grant ER-15522. Use was made of the IMSERC X-ray Facility at Northwestern University, supported by the International Institute of Nanotechnology. This work was supported by the Director, Office of Science, Office of Basic Energy Sciences, Division of Chemical Sciences, Geosciences, and Biosciences of the U.S. Department of Energy under Contract DE-AC02-05CH11231 at Lawrence Berkeley National Laboratory (LBNL). The Molecular Environmental Sciences Beamline 11.0.2 at the Advanced Light Source was supported by the Condensed Phase and Interfacial Molecular Sciences Program of the aforementioned Division of the U.S. Department of Energy under Contract No. DE-AC02-05CH11231 at LBNL. The Advanced Light Source is supported by the Director, Office of Science, Office of Basic Energy Sciences, of the U.S. Department of Energy under Contract No. DE-AC02-05CH11231 at LBNL. A portion of this work was performed at the National High Magnetic Field Laboratory, which is supported by NSF Cooperative Agreement No. DMR-1157490 by the State of Florida and by the DOE.

REFERENCES

(1) Narducci, A. A.; Ibers, J. A. *Chem. Mater.* **1998**, *10*, 2811−2823.
(2) Manos, E.; Kanatzidis, M. G.; Ibers, J. A. In *The Chemistry of the Actinide and Transactinide Elements*, 4th ed.; Morss, L. R.; Edelstein, N. M.; Fuger, J., Eds.; Springer: Dordrecht, The Netherlands, 2010; Vol. *6*, pp 4005−4078.
(3) Rodier, N.; Tien, V. *Acta Crystallogr. Sect. B: Struct. Crystallogr. Cryst. Chem.* **1976**, *32*, 2705−2707.
(4) Julien, R.; Rodier, N.; Tien, V. *Acta Crystallogr. Sect. B: Struct. Crystallogr. Cryst. Chem.* **1978**, *34*, 2612−2614.
(5) Prakash, J.; Ibers, J. A. *Structure of $ScUS_3$*, unpublished.
(6) Stöwe, K. *J. Solid State Chem.* **1996**, *127*, 202−210.
(7) Moseley, P. T.; Brown, D.; Whittaker, B. *Acta Crystallogr.* **1972**, *B28*, 1816−1821.
(8) Noël, H.; Prigent, J. *Physica B+C* **1980**, *102*, 372−379.
(9) Tougait, O.; Potel, M.; Noël, H. *J. Solid State Chem.* **1998**, *139*, 356−361.
(10) Daoudi, A.; Potel, M.; Noël, H. *J. Alloys Compd.* **1996**, *232*, 180−185.
(11) Daoudi, A.; Noël, H. *Inorg. Chim. Acta* **1986**, *117*, 183−185.
(12) Noël, H.; Padiou, J.; Prigent, J. *C. R. Seances Acad. Sci., Ser. C* **1971**, *272*, 206−208.
(13) Noël, H. *C. R. Seances Acad. Sci., Ser. C* **1973**, *277*, 463−464.
(14) Noël, H. *C. R. Seances Acad. Sci., Ser. C* **1974**, *279*, 513−515.
(15) Noël, H.; Potel, M.; Padiou, J. *Acta Crystallogr. Sect. B: Struct. Crystallogr. Cryst. Chem.* **1975**, *31*, 2634−2637.
(16) Kohlmann, H.; Stöwe, K.; Beck, H. P. *Z. Anorg. Allg. Chem.* **1997**, *623*, 897−900.
(17) Oh, G. N.; Ibers, J. A. *Acta Crystallogr.* **2011**, *E67*, i46.
(18) Vovan, T.; Rodier, N. *C. R. Seances Acad. Sci., Ser. C* **1979**, *289*, 17−20.
(19) Noel, H.; Troc, R. *J. Solid State Chem.* **1979**, *27*, 123−135.
(20) Bugaris, D. E.; Ibers, J. A. *J. Solid State Chem.* **2008**, *181*, 3189−3193.
(21) Haneveld, A. J. K.; Jellinek, F. *J. Less-Common Met.* **1969**, *18*, 123−129.
(22) Ward, M. D.; Oh, G. N.; Ibers, J. A. *Structure of $Cs_2U_6M_2Se_{15}$ (M = Ti, Cr)*. Unpublished.
(23) *Bruker APEX2 Version 2009.5−1 Data Collection and Processing Software*; Bruker Analytical X-Ray Instruments, Inc.: Madison, WI, USA, 2009.
(24) Sheldrick, G. M. *SADABS*; Department of Structural Chemistry, University of Göttingen: Göttingen, Germany, 2008.
(25) Sheldrick, G. M. *TWINABS*; University of Göttingen: Göttingen, Germany, 2008.
(26) Sheldrick, G. M. *Acta Crystallogr. Sect. A: Found. Crystallogr.* **2008**, *64*, 112−122.
(27) Gelato, L. M.; Parthé, E. *J. Appl. Crystallogr.* **1987**, *20*, 139−143.
(28) Palmer, D. *CrystalMaker Software*, Version 2.7.7; CrystalMaker Software Ltd.: Oxford, England, 2013.
(29) Bluhm, H.; Andersson, K.; Araki, T.; Benzerara, K.; Brown, G. E.; Dynes, J. J.; Ghosal, S.; Gilles, M. K.; Hansen, H.-C.; Hemminger, J. C.; Hitchcock, A. P.; Ketteler, G.; Kilcoyne, A. L. D.; Kneedler, E.; Lawrence, J. R.; Leppard, G. G.; Majzlam, J.; Mun, B. S.; Myneni, S. C. B.; Nilsson, A.; Ogasawara, H.; Ogletree, D. F.; Pecher, K.; Salmeron, M.; Shuh, D. K.; Tonner, B.; Tyliszczak, T.; Warwick, T.; Yoon, T. H. *J. Electron Spectrosc. Relat. Phenom.* **2006**, *150*, 86−104.
(30) Gianetti, T. L.; Nocton, G.; Minasian, S. G.; Tomson, N. C.; Kilcoyne, A. L. D.; Kozimor, S. A.; Shuh, D. K.; Tyliszczak, T.; Bergman, R. G.; Arnold, J. *J. Am. Chem. Soc.* **2013**, *135*, 3224−3236.
(31) Minasian, S. G.; Keith, J. M.; Batista, E. R.; Boland, K. S.; Bradley, J. A.; Daly, S. R.; Kozimor, S. A.; Lukens, W. W.; Martin, R. L.; Nordlund, D.; Seidler, G. T.; Shuh, D. K.; Sokaras, D.; Tyliszczak, T.; Wagner, G. L.; Weng, T.-C.; Yang, P. *J. Am. Chem. Soc.* **2013**, *135*, 1864−1871.
(32) Minasian, S. G.; Keith, J. M.; Batista, E. R.; Boland, K. S.; Kozimor, S. A.; Martin, R. L.; Shuh, D. K.; Tyliszczak, T.; Vernon, L. J. *J. Am. Chem. Soc.* **2013**, *135*, 14731−14740.
(33) Bugaris, D. E.; Choi, E. S.; Copping, R.; Glans, P.-A.; Minasian, S. G.; Tyliszczak, T.; Kozimor, S. A.; Shuh, D. K.; Ibers, J. A. *Inorg. Chem.* **2011**, *50*, 6656−6666.
(34) Minasian, S. G.; Krinsky, J. L.; Rinehart, J. D.; Copping, R.; Tyliszczak, T.; Janousch, M.; Shuh, D. K.; Arnold, J. *J. Am. Chem. Soc.* **2009**, *131*, 13767−13783.
(35) Minasian, S. G.; Keith, J. M.; Batista, E. R.; Boland, K. S.; Clark, D. L.; Kozimor, S. A.; Martin, R. L.; Shuh, D. K.; Tyliszczak, T. *Chem. Sci.* **2014**, *5*, 351−359.
(36) Kresse, G.; Forthmüller, J. *Comput. Mater. Sci.* **1996**, *6*, 15−50.
(37) Kresse, G.; Joubert, D. *Phys. Rev. B* **1999**, *59*, 1758−1775.
(38) Hohenberg, P.; Kohn, W. *Phys. Rev.* **1964**, *136*, 864−871.
(39) Kohn, W.; Sham, L. J. *Phys. Rev.* **1965**, *140*, 1133−1138.
(40) Blöchl, P. E. *Phys. Rev. B* **1994**, *50*, 17953−17979.
(41) Perdew, J. P.; Burke, K.; Ernzerhof, M. *Phys. Rev. Lett.* **1996**, *77*, 3865−3868.
(42) Jin, G. B.; Ringe, E.; Long, G. J.; Grandjean, F.; Sougrati, M. T.; Choi, E. S.; Wells, D. M.; Balasubramanian, M.; Ibers, J. A. *Inorg. Chem.* **2010**, *49*, 10455−10467.
(43) Noël, H.; Padiou, J.; Prigent, J. *C. R. Seances Acad. Sci., Ser. C* **1975**, *280*, 123−126.
(44) Shannon, R. D. *Acta Crystallogr. Sect. A: Cryst. Phys. Diffr. Theor. Gen. Crystallogr.* **1976**, *32*, 751−767.
(45) Noël, H. *J. Solid State Chem.* **1984**, *52*, 203−210.
(46) Spek, A. L. *PLATON, A Multipurpose Crystallographic Tool*; Utrecht University: Utrecht, The Netherlands, 2014.
(47) Brese, N. E.; O'Keeffe, M. *Acta Crystallogr. Sect. B: Struct. Sci.* **1991**, *47*, 192−197.
(48) de Groot, F. M. F.; Fuggle, J. C.; Thole, B. T.; Sawatzky, G. A. *Phys. Rev. B* **1990**, *41*, 928−937.
(49) Aquila, A. L.; Salmassi, F.; Gullikson, E. M. *Proc. SPIE Int. Soc. Opt. Eng.* **2004**, *5538*, 64−71.
(50) Shendruk, T. N.; Moewes, A.; Kurmaev, E. Z.; Ochin, P.; Maury, H.; André, J. M.; Le Guen, K.; Jonnard, P. *Thin Solid Films* **2010**, *518*, 3808−3812.

(51) Bradley, J. A.; Moore, K. T.; van der Laan, G.; Bradley, J. P.; Gordon, R. A. *Phys. Rev. B* **2011**, *84*, 205105.
(52) Nilsson, H. J.; Tyliszczak, T.; Wilson, R. E.; Werme, L.; Shuh, D. K. *Anal. Bioanal. Chem.* **2005**, *383*, 41−47.
(53) Janousch, M.; Copping, R.; Tyliszczak, T.; Castro-Rodriguez, I.; Shuh, D. K. *Mater. Res. Soc. Symp. Proc.* **2008**, *1104*, 165−170.
(54) van der Laan, G.; Moore, K. T.; Tobin, J. G.; Chung, B. W.; Wall, M. A.; Schwartz, A. J. *Phys. Rev. Lett.* **2004**, *93*, 097401.
(55) Tobin, J. G.; Moore, K. T.; Chung, B. W.; Wall, M. A.; Schwartz, A. J.; van der Laan, G.; Kutepov, A. L. *Phys. Rev. B* **2005**, *72*, 085109.
(56) Moore, K. T.; van der Laan, G.; Haire, R. G.; Wall, M. A.; Schwartz, A. J. *Phys. Rev. B* **2006**, *73*, 033109.
(57) Moore, K. T.; van der Laan, G. *Rev. Mod. Phys.* **2009**, *81*, 235−298.
(58) Bugaris, D. E.; Copping, R.; Tyliszczak, T.; Shuh, D. K.; Ibers, J. A. *Inorg. Chem.* **2010**, *49*, 2568−2575.
(59) Sechovsky, V.; Havela, L. In *Handbook of Magnetic Materials*, 1st ed.; Buschow, K. H. J., Ed.; Elsevier: Amsterdam, 1998; Vol. *11*, pp 1−290.

dx.doi.org/10.1021/ic500721d | *Inorg. Chem.* 2014, 53, 6920−6927